Vol 17 No 5, May 2008
1674-1056/2008/17(05)/1854-04
Chinese Physics B
© 2008 Chin. Phys. Soc.
and IOP Publishing Ltd

Resonant detection of terahertz radiation utilizing plasma waves in high-electron-mobility transistors*

Ma Ming-Rui(马明瑞), Chen Yu-Ling(陈钰玲), Wang Li-Min(王立敏), and Wang Chang(王 长)†

State Key Laboratory of Functional Materials for Informatics, Shanghai Institute of Microsystem and Information Technology, Chinese Academy of Sciences and Graduate School of Chinese Academy of Sciences, Shanghai 200050, *China*

(Received 16 May 2007; revised manuscript received 24 August 2007)

This paper theoretically studies the high-electron-mobility transistor (HEMT) driven by the terahertz radiation. It calculates the gate-to-source/drain admittance and the detection responsivity of the HEMT as a function of the signal frequency. It finds that the peaks of the admittances and the responsivity show redshift, and the heights of the peaks decrease with increasing the lengths of the source-to-gate and gate-to-drain spacing. Such phenomena may be useful in designing different HEMTs by utilizing the effects associated with the plasma oscillations excitation.

Keywords: terahertz radiation, resonant, HEMT
PACC: 5265, 7230, 7340N

1. Introduction

Recently, terahertz (THz) plasma effects in high-electron-mobility transistors (HEMTs) have attracted a growing interest of theoretical[1−13] and experimental[14−23] studies. Plasma wave is the oscillation of electron density in time and space, and the channel of a field-effect transistor with sufficiently high electron mobility can serve as a resonant cavity for the plasma wave. Moreover when a certain relation between the signal frequency and the electron transit time is fulfilled, the self-excitation of plasma oscillations can occur in HEMT-like heterostructures with tunnelling or thermionic electron injection from the channel into the gate layer, and its typical plasma frequencies $\omega_{\rm p}$ lie in the THz range. Such phenomena can be used for generation, detection, mixing, and frequency multiplication of THz radiation.

The principle of the HEMT operation as a detector is described in the following. The signal component of the voltage created by the THz radiation is applied to the side contacts to the HEMT channel. It excites a standing plasma wave in the latter. The oscillating electric potential of channel determines the AC component of the emitter-collector channel. When the signal frequency is close to one of the resonant plasma frequencies, the amplitude of the oscillating potential in the channel can be larger than the amplitude of the incoming signal. Due to the nonlinear dependence of the current density through the channel into the gate and the channel local potential, the variation of current contains the component at the frequency of the incoming signal, its harmonics and the rectified component.

A lot of work has been done in the field of HEMT plasma detector. However, the effects of the length of the contact region need further study. In this paper, we use the model developed by Satou *et al*[13] to study the HEMT driven by the THz radiation. We theoretically show that the peaks of the admittances and the responsivities show redshift, and the heights of the peaks decrease with increasing the lengths of the source-to-gate and gate-to-drain spacings. Such phenomena can be useful in designing different HEMT by utilizing the effects associated with the plasma oscillations excitation.

2. Basic equations of the physical model

The HEMT considered here has an undoped channel formed at the heterointerface between wide-gap

*Project supported by the National Fund for Distinguished Young Scholars of China (Grant No 60425415), the National Science Foundation of China (Grant No 60721004), the Shanghai Municipal Commission of Science and Technology, China (Grant Nos 06DJ14008 and 06CA07001), and the National Basic Research Program of China (Grant No 2007CB310402).
†Corresponding author. E-mail: cwang@mail.sim.ac.cn

(AlGaAs) and narrow-gap (GaAs) layers, and the side contacts to the channel (source and drain) are connected (see Fig.1). It assumes that the structural parameters and the bias gate voltage are chosen to provide an effective electron injection from the channel into the gate layer through tunnelling.

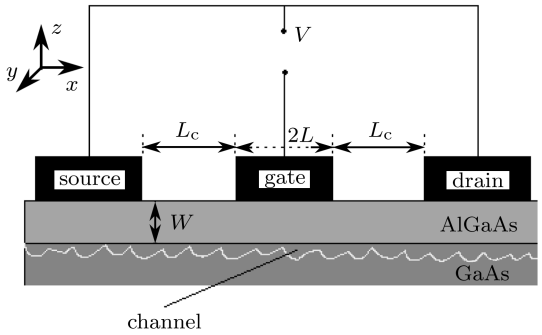


Fig.1. Schematic view of the HEMT structure.

Assume that a small AC voltage $V(t) = \delta V\omega\exp(\text{-i}\omega t)$, where $\delta V\omega$ and ω are respectively the signal amplitude and frequency, is applied between the contacts. The electron sheet concentration $\Sigma(x,t) = \Sigma_0 + \delta\Sigma\omega(x)\exp(\text{-i}\omega t)$, the electron velocity along the channel $u(x,t) = u_0 + \delta u\omega\exp(\text{-i}\omega t)$ and electric potential of the 2D channel $\varphi(x,t) = \varphi_0 + \delta\varphi\omega\exp(\text{-i}\omega t)$, where subscript 0 denotes the steady-state values and subscript ω denotes the small-signal amplitudes corresponding to the frequency ω, obey the continuity equation and the Euler equation:[11−13]

$$\frac{\partial\sum}{\partial t} + \frac{\partial\sum u}{\partial x} = \frac{j}{e}, \tag{1}$$

$$\frac{\partial u}{\partial t} + u\frac{\partial u}{\partial x} + \nu u = \frac{e}{m}\frac{\mathrm{d}\varphi_\omega}{\mathrm{d}x}, \tag{2}$$

here e is the electron charge, m is the electron effective mass, ν is the electron collision frequency, and $j = j(\xi)$ is the density of the electron leakage current from the channel into the gate, with $\xi = -4\pi e\Sigma/\varepsilon$ and ε is the dielectric constant.

For small amplitudes of the incoming signals, one can present the variation of the electric field at the heterointerface $\delta\xi$ in the form[13]

$$\delta j \simeq \sigma\delta\xi + \beta\delta\xi^2 + \gamma\delta\xi^3 + \cdots, \tag{3}$$

where σ is the differential conductivity associated with the electron tunnelling injection from the channel into the gate layer, and parameters β and γ characterize the nonlinearity. Assuming that $j(\xi) = -e\nu_{\mathrm{QW}}\Sigma\exp(\text{-}E_t/|\xi|)$, one can get $\sigma = (\varepsilon\nu_{\mathrm{QW}}/4\pi)(1 + E_t/|\xi_0|)\exp(\text{-}E_t/|\xi_0|)$, and $\beta = -(\varepsilon\nu_{\mathrm{QW}}/8\pi)(E_t^2/|\xi_0|^3)\exp(-E_t/|\xi_0|)$. Where $E_t = 4(2m\varepsilon_0^3)^{1/2}/3e\hbar$, $\hbar$ is the reduced Planck constant, and ε_0 is the conduction band offset at the heterointerface, $|\xi_0| = V_0/W$.

Introducing the electron transit time across the gate layer $\tau_d = W/v_d$ and the characteristic injection frequency $\nu_t = 4\pi\sigma/\varepsilon$ (here v_d is the electron drift velocity across the gate layer), solving the Poisson equation in the gate layer, we can express the AC component of the electron sheet concentration in the channel in terms of φ_ω as follows[13]

$$\Sigma_\omega = -\frac{\varepsilon}{4\pi eW}c_\omega\varphi_\omega, \tag{4}$$

where $c_\omega = [1 + \mathrm{i}\nu_t/\omega - \mathrm{i}\nu_t f(\omega\tau_d)/\omega]^{-1}$, and $f(\omega\tau_d) = [\exp(\mathrm{i}\omega\tau_d) - 1]/(\mathrm{i}\omega\tau_d)$.

Using Eqs.(1), (2) and (4), we can get the following equation for φ_ω in the region beneath the gate ($|x| \le L$):

$$\frac{\mathrm{d}^2\delta\varphi_\omega}{\mathrm{d}x^2} + s^{-2}c_\omega u_0\left(\upsilon - \mathrm{i}\omega\right)\frac{\mathrm{d}\delta\varphi_\omega}{\mathrm{d}x} + s^{-2}\left(\omega + \mathrm{i}\upsilon\right)\left(\omega + \mathrm{i}\upsilon_t\right)c_\omega\delta\varphi_\omega = 0, \tag{5}$$

here $s = (4\pi e^2\Sigma_0 W/\varepsilon m)^{1/2} = (eV_0/m)^{1/2}$ is the plasma wave velocity.

The boundary condition can be taken in the following form:[13]

$$\delta\varphi_\omega|_{x=\pm L} = \delta V_\omega \mp L_\omega\frac{\mathrm{d}\delta\varphi_\omega}{\mathrm{d}x}|_{x=\pm L}, \tag{6}$$

where $L_\omega = L_c(\Sigma_0/\Sigma_{0c})(\nu_c - \mathrm{i}\omega)/(\nu - \mathrm{i}\omega)$, Σ_{0c} and ν_c are the electron sheet concentration and the electron collision frequency in the contact regions.

Using Eq.(5) with boundary conditions (6), we obtain

$$\delta\varphi_\omega = c_1\exp\left(\lambda_1 x\right) + c_2\exp\left(\lambda_2 x\right), \tag{7}$$

here

$$\lambda_1 = \frac{-b + \sqrt{b^2 - 4c}}{2}, \tag{8}$$

$$\lambda_2 = \frac{-b - \sqrt{b^2 - 4c}}{2}, \tag{9}$$

$$c_1 = \frac{\delta V_\omega \left(\dfrac{\exp(-\lambda_2 L)}{1+L_\omega \lambda_2} - \dfrac{\exp(\lambda_2 L)}{1-L_\omega \lambda_2} \right)}{\exp(\lambda_1 - \lambda_2) L \dfrac{1+L_\omega \lambda_1}{1+L_\omega \lambda_2} - \exp(\lambda_2 - \lambda_1) L \dfrac{1-L_\omega \lambda_1}{1-L_\omega \lambda_2}}, \tag{10}$$

$$c_2 = \frac{\delta V_\omega \left(\dfrac{\exp(-\lambda_1 L)}{1+L_\omega \lambda_1} - \dfrac{\exp(\lambda_1 L)}{1-L_\omega \lambda_1} \right)}{\exp(\lambda_2 - \lambda_1) L \dfrac{1+L_\omega \lambda_2}{1+L_\omega \lambda_1} - \exp(\lambda_1 - \lambda_2) L \dfrac{1-L_\omega \lambda_2}{1-L_\omega \lambda_1}}, \tag{11}$$

where $b = u_0 s - 2c\omega(v - \mathrm{i}\omega)$, $c = s - 2c\omega(\omega + \mathrm{i}v)(\omega + \mathrm{i}vt)$.

3. Calculation of admittance and detection responsivity

The net AC current (per unit length) is given by

$$\delta J_\omega = \left(\sigma - \mathrm{i}\frac{\omega\varepsilon}{4\pi}\right) \frac{c_\omega}{W} \int_{-L}^{L} \mathrm{d}x \delta\varphi_\omega, \tag{12}$$

substituting $\delta\varphi_\omega$ from Eq.(7) into Eq.(12) and integrating, we obtain

$$\delta J_\omega = \delta V_\omega \left(\sigma - \mathrm{i}\frac{\omega\varepsilon}{4\pi}\right) \frac{c_\omega}{W} \left\{ \frac{c_1}{\lambda_1} [\exp(\lambda_1 L) - \exp(-\lambda_1 L)] + \frac{c_2}{\lambda_2} [\exp(\lambda_2 L) - \exp(-\lambda_2 L)] \right\}. \tag{13}$$

Equation (13) yields the gate-to-source/drain admittance of the HEMT:

$$Y_\omega = \left(\sigma - \mathrm{i}\frac{\omega\varepsilon}{4\pi}\right) \frac{c_\omega}{W} \left\{ \frac{c_1}{\lambda_1} [\exp(\lambda_1 L) - \exp(-\lambda_1 L)] + \frac{c_2}{\lambda_2} [\exp(\lambda_2 L) - \exp(-\lambda_2 L)] \right\}. \tag{14}$$

Figure 2 shows the frequency dependences of the real and imaginary parts of the admittance with different lengths of the source-to-gate and gate-to-drain spacings. The parameters used in Fig.2 were chosen as follows: $L = 0.25\,\mu$m, $W = 0.05\,\mu$m, $\nu_{\mathrm{QW}} = 1 \times 10^{13}\,\mathrm{s}^{-1}$, $v_{\mathrm{d}} = 1 \times 10^7\,$cm/s, $L_\omega = L_{\mathrm{c}}$ (i.e., $\Sigma_{0\mathrm{c}} = \Sigma_0$ and $\nu_{\mathrm{c}} = v$), $v_{\mathrm{d}} = 1 \times 10^7\,$cm/s, $V_0 = 0.75\,V$, and $v = 1 \times 10^{12}\,\mathrm{s}^{-1}$. One can see that with the increase of lengths of the source-to-gate and gate-to-drain spacings, the peaks of the admittance show redshift, and the height of the peaks decreases. So we can find out that plasma oscillations become weaker when the lengths of source-to-gate and gate-to-drain spacings increase.

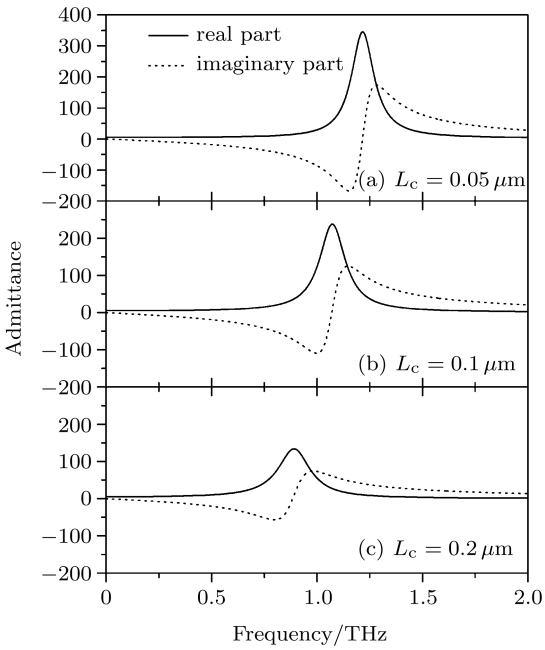


Fig.2. Real (solid) and imaginary (dot) parts of the HEMT gate-to-source/drain admittance versus signal frequency for different lengths of the contact regions (collision frequency set as $\nu = 1 \times 10^{12}\mathrm{s}^{-1}$).

From Eq.(7) we obtain

$$\mathrm{Re}\delta\varphi = |A_\omega(x)| \cos(\omega t - \theta_\omega), \tag{15}$$

here

$$|A_\omega| = |c_1 \exp(\lambda_1 x) + c_2 \exp(\lambda_2 x)|. \tag{16}$$

Using Eqs.(3) and (13), after averaging over the signal period we obtain the following expression for the current component induced by incoming signal:

$$\delta J_0 = \frac{\beta \left|c_\omega\right|^2}{2W^2} \int_{-L}^{L} \mathrm{d}x \left|A_\omega\left(x\right)\right|^2. \qquad (17)$$

Figure 3 illustrates the frequency dependence of the responsivity associated with the nonlinear response $\delta J_0/\delta V_\omega^2$, the value proportional to the rectified component of the current. The parameter used in

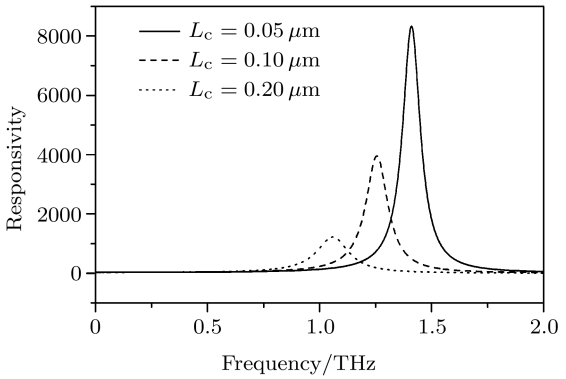


Fig.3. Detection responsivity versus signal frequency for different lengths of the contact regions (collision frequency set as $\nu = 1 \times 10^{12}\,\mathrm{s}^{-1}$, electron drift velocity across the gate layer $v_\mathrm{d} = 1 \times 10^7\,\mathrm{cm/s}$, $V_0 = 1.0\,\mathrm{V}$).

Fig.3 is chosen to be $\varepsilon_0 = 0.1\,\mathrm{eV}$ which corresponds to $V_\mathrm{t} = 2.92\,\mathrm{V}$. The other parameters are the same as those listed above. One can see that with the increase of lengths of the source-to-gate and gate-to-drain spacings, the peaks of the responsivity show redshift, and the height of the peaks decreases. The resonant peaks of the detection responsivity are associated with the coincidence of the incoming THz radiation frequency and the resonant plasma frequency. The shift of the peak position with changing the lengths of the source-to-gate and gate-to-drain spacings is attributed to the change of the electron concentration in the channel and matching of the plasma and transit-time resonances.

4. Conclusions

In summary, we calculate the gate-to-source/drain admittance and the detection responsivity of the HEMT as a function of the signal frequency. It shows that with the increase of lengths of the source-to-gate and gate-to-drain spacings, the electron concentration in the channel changes, the matching of the plasma and transit-time resonances also changes, which induce the peaks of the admittance and the responsivity red shift, and the height of the peaks decreases. In order to gain a good performance of the detector, we should make the lengths of the source-to-gate and gate-to-drain spacings as short as possible.

Acknowledgments

The authors would like to thank Guo X G and Lü J T for many helpful discussions.

References

[1] Chaplik A V 1972 *Sov. Phys. JETP* **35** 396
[2] Dyakonov M and Shur M 1993 *Phys. Rev. Lett.* **71** 2465
[3] Dyakonov M and Shur M 1993 *Phys. Rev.* B **51** 14341
[4] Cao J C 2003 *Phys. Rev. Lett.* **91** 237401
[5] Mi X W, Cao J C and Zhang C 2004 *J. Appl. Phys.* **95** 1191
[6] Cao J C and Lei X L 2003 *Phys. Rev.* B **67** 085309
[7] Cao J C and Lei X L 1999 *Phys. Rev.* B **60** 1871
[8] Cao J C, Lei X L, Li A Z and Liu H C 2001 *Appl. Phys. Lett.* **78** 2524
[9] Cao J C, Liu H C and Lei X L 2000 *J. Appl. Phys.* **87** 2867
[10] Rudin S and Samsonidze G 1999 *J. Appl. Phys.* **86** 2083
[11] Ryzhii V and Shur M 2002 *Semicond. Sci. Technol.* **17** 1168
[12] Ryzhii V, Satou A, Khmyrova I, Chapik A and Shur M 2004 *J. Appl. Phys.* **98** 12
[13] Satou A, Khmyrova I, Ryzhii V and Shur M 2003 *Semicond. Sci. Technol.* **18** 460
[14] Lü J Q, Shur M S, Hesler J L, Sun L and Weikle R 1998 *IEEE Electron Device Lett.* **19** 373
[15] Weikle R, Lü J Q, Shur M S and Dyakonov M 1996 *Electron. Lett.* **32** 2148
[16] Lü J Q and Shur M S 2001 *Appl. Phys. Lett.* **78** 2587
[17] Liu H C, Song C Y, SpringThorpe A J and Cao J C 2004 *Appl. Phys. Lett.* **84** 4068
[18] Liu H C, Song C Y, Wasilewski Z R, SpringThorpe A J, Cao J C, Dharmawardana C, Aers G C, Lockwood D J and Gupta J A 2003 *Phys. Rev. Lett.* **90** 077402
[19] Knap W, Deng Y, Rumyantsev S, Lü J Q, Shur M S, Saylor C A and Brunel L C 2002 *Appl. Phys. Lett.* **80** 3433
[20] Knap W, Deng Y, Rumyantsev S and Shur M S 2002 *Appl. Phys. Lett.* **81** 4637
[21] Li W, Gao H, Gong M L and Liu S G 2004 *Chin. Phys.* **13** 114
[22] Zhang J T 2005 *Chin. Phys.* **14** 169
[23] Guo W, Ouyang J M, Shao F Q and Wang L 2004 *Chin. Phys.* **13** 2174